

SUPPORT EFFECT ON CONVERSION OF QUINOLINE OVER ReS_2 CATALYST

R. BASSI^a, M. VILLARROEL^b, F. J. GIL-LLAMBIAS^b, P. BAEZA^a, J. L. GARCÍA-FIERRO^c, N. MARTÍNEZ^d,
P. OLIVERA^d, K. LEIVA^d, N. ESCALONA^{e, f, g*}

^a Pontificia Universidad Católica de Valparaíso, Facultad de Ciencias, Instituto de Química, Casilla 4059, Valparaíso, Chile.

^b Universidad de Santiago de Chile, Casilla 40, Correo 33, Santiago, Chile

^c Instituto de Catálisis y Petroquímica, CSIC, Cantoblanco, 28049 Madrid, Spain.

^d Universidad de Concepción, Facultad de Ciencias Químicas, Casilla 160C, Concepción, Chile.

^e Departamento de Ingeniería Química y Bioprocesos, Escuela de Ingeniería, Pontificia Universidad Católica de Chile, Avenida Vicuña Mackenna 4860, Macul, Santiago, Chile.

^f Departamento de Química Física, Facultad de Químicas, Pontificia Universidad Católica de Chile.

^g Centro de Investigación en Nanotecnología y Materiales Avanzados (CIEN-UC), Pontificia Universidad Católica de Chile, Santiago, Chile.

ABSTRACT

The conversion of quinoline over ReS_2 supported on $\gamma\text{-Al}_2\text{O}_3$, SiO_2 , ZrO_2 and TiO_2 catalysts in a batch reactor at 300°C and 5 MPa of hydrogen pressure was studied. The catalysts were prepared by wet impregnation with a loading of 1.5 atoms of Re per nm^2 of support. The catalysts were characterized by N_2 adsorption, X-ray photoelectron spectroscopy (XPS) and X-ray powder diffraction (XRD). The $\text{Re}(x)/\text{supports}$ catalysts displayed high activities for the conversion of quinoline, although negligible formation of N-free compounds (hydrodenitrogenation) were observed. The intrinsic activities of ReS_2 were modified by the support decreased in the order: $\text{Re}/\text{TiO}_2 > \text{Re}/\text{ZrO}_2 > \text{Re}/\text{SiO}_2 > \text{Re}/\gamma\text{-Al}_2\text{O}_3$. The highest activity displayed by the Re/TiO_2 catalyst was correlated with the Re dispersion and formation of ReS_2 species. Meanwhile, the lower conversion of quinoline over the Re/ZrO_2 , Re/SiO_2 and $\text{Re}/\gamma\text{-Al}_2\text{O}_3$ catalysts was related to the combined effect of the textural properties of catalysts and the formation of $\text{ReS}_{(2-x)}$ species on the supports.

Keywords: Hydrodenitrogenation, ReS_2 , quinoline, supports.

1. INTRODUCTION

Recently, the quality of crude oil has declined due to the contents of heavier nitrogen and sulfur organic compounds which hinder the hydrotreating processes (HT), particularly hydrodesulfurization (HDS) and hydrodenitrogenation (HDN). Moreover, stringent environmental regulations have forced the oil industry to reduce the nitrogen and sulfur levels present in fuels. In order to meet the required standards, it is essential to find catalysts that are more active than the classical HT $\text{Ni}(\text{Co})\text{-Mo}/\text{Al}_2\text{O}_3$ catalysts. In this context, several researches have been carried out in order to either improve the activity of classical sulfides catalysts or find alternative catalysts [1, 2, 3].

Liu *et al.* [1] studied the effects of the addition of fluorine and phosphorus on $\text{Ni-Mo}/\text{Al}_2\text{O}_3$ catalysts in the HDN of quinoline. They found that fluorine and phosphorus promote the activity of $\text{Ni-Mo}/\text{Al}_2\text{O}_3$ catalysts, attributing this behavior to the promotion of weak and moderate acid sites, as well as the enhancement of Mo dispersion.

Deepa *et al.* [4] investigated the effect of supports on the HDN of quinoline and 1,2,3,4-tetrahydroquinoline (THQ1) over Ni-Mo catalysts. The highest quinoline conversion was displayed by Ni-Mo supported on a B-zeolite dealuminated blend with Al_2O_3 ($\text{Al}_2\text{O}_3\text{-DAI BEA-Al}$), followed by $\text{Ni-Mo}/\text{Al}_2\text{O}_3$ catalyst. On the other hand, the highest THQ1 conversion was presented by $\text{Ni-Mo}/\text{Al}_2\text{O}_3$ (DAI BEA-AL), followed by $\text{Ni-Mo}/\text{AIMCM-41}$ catalyst. The trend obtained was attributed mainly to differences in the acid strength of supports used.

Yang and Satterfield [5] studied the effect of hydrogen sulfide on the HDN of quinoline using $\text{NiMo}/\text{Al}_2\text{O}_3$ catalyst. They found that the hydrogen sulfide inhibits hydrogenation and dehydrogenation reactions but markedly accelerates hydrogenolysis reactions.

Moreau *et al.* [6] studied HDN of quinoline using mechanical mixtures of industrial pre-sulfided alumina-supported Ni-Mo and Co-Mo catalysts. They found a substantial promotion effect, due mainly to the better hydrogenolysis properties of the catalysts mixtures. The authors indicated that this effect could be due to a novel active phase or due to a bifunctional mechanism.

The reactivity of non-classical catalysts has also been studied for HDN and HDS reactions. Ni-rich bimetallic phosphides incorporating different metals displayed high activity in the simultaneous HDN of quinoline and HDS of dibenzothiophene [2]. However, the HDS conversion and product selectivities were dependent on the adsorption of N-containing compounds on the active sites of catalysts [7, 8]. These results reiterated that the removal of nitrogen from heterocyclic compounds is a more difficult process than the removal of sulfur, and generally leads to deactivation of catalysts.

Chouzier *et al.* [9] studied (Ni, Co)-Mo binary and ternary nitrides in the HDN of quinoline. They found that the active phase for monometallic nitrides was MoS_2 formed on the surface of nitride particles. This was confirmed by the poor activity of the nitride in the absence of sulfur. The authors reported synergism for these bimetallic nitride systems, and indicated that the active sites are probably some ensembles of metallic atoms on the surface of mixed phases $\text{Co}_3\text{Mo}_3\text{N}$ and $\text{Ni}_3\text{Mo}_3\text{N}$.

On the other hand, Eijsbouts *et al.* [10] studied the reactivities of first-, second-, and third-row transition metal sulfide (TMS) supported on activated carbon in the HDN of quinoline. They found that the first-row transition metal sulfides displayed low quinoline conversion to hydrocarbons. On the other hand, the second- and third-row TMS formed a volcanic curve with maxima at Rh/C and Ir/C catalysts, respectively. On this curve, Re/C presented intermediate activity but with a high selectivity for propylbenzene. The ReS_2 catalyst has been rarely studied for HDN reactions although a $\text{ReS}_2/\text{Al}_2\text{O}_3$ catalyst exhibited a higher activity (1.6 times) than the $\text{Ni-Mo}/\text{Al}_2\text{O}_3$ catalyst in the HDS of thiophene [11].

Escalona *et al.* [12] studied the simultaneous HDS and HDN reaction over $\text{ReS}_2/\text{Al}_2\text{O}_3$ catalyst. They found that the HDN/HDS selectivity increases with increasing Re loading, which was attributed to changes in the acid sites of the catalysts. A similar behavior was also observed in the simultaneous HDS and HDN over ReS_2/C catalysts [13].

On the other hand, Laurenti *et al.* [14] studied the HDS of thiophene over ReS_2 supported on Al_2O_3 , ZrO_2 and TiO_2 . They found that the $\text{ReS}_2/\text{ZrO}_2$ catalyst displayed the highest activity followed by $\text{ReS}_2/\text{Al}_2\text{O}_3$ and $\text{ReS}_2/\text{TiO}_2$ catalysts, and that catalytic activity was strongly dependent on the sulfidation mixture used, similar to previous findings by Escalona *et al.* [11].

It is well known that the activity of transition metal sulfides strongly depends on the type of support used. The support can influence the interaction between its surface and the active phase, the dispersion, degree of sulfuration, stability, and structure of the active phase, etc. [15, 16, 17, 18]. Therefore, the aim of this work is to study the effect of support (TiO_2 , Al_2O_3 , SiO_2 and ZrO_2) on conversion of quinoline using Re sulfide as active phase. The preparation of Re sulfide catalysts was carried out with $\text{N}_2/\text{H}_2\text{S}$ mixture, following a procedure previously reported by Escalona *et al.* [14].

2.- EXPERIMENTAL

2.1 Catalyst preparation

The supported rhenium-based catalysts were prepared by incipient wetness impregnation of an aqueous solution of NH_4ReO_4 (Aldrich, 99%) on

SiO₂ (BASF D10-11), γ -Al₂O₃ (BASF D10-10), TiO₂ (p25 Degussa) and ZrO₂. The ZrO₂ support was obtained by direct calcination of a commercial hydrous zirconium Zr(OH)₄ (MEL Chemicals) at 573 K for 3 h in a muffle furnace. The catalysts were prepared with a loading 1.5 atoms of Re per nm² of support. The impregnated catalysts were left for maturation at room temperature for 24 h, dried at 393 K for 12 h, and then calcined at 573 K for 0.5 h. The calcined samples were pre-sulfided at 673 K for 4 h under a flow of 10 % H₂S/N₂ mixture. The Re content was determined by ICP-OES using the Re emission line of 221.426 nm.

2.2 Characterization of the Catalysts

The BET surface area (S_{BET}) and total pore volume (V_p) of the support and the ReOx/support catalysts were determined from nitrogen isotherms at 77 K using a Micromeritics-TriStar II 3020 instrument.

X-ray powder diffraction (XRD) patterns were obtained by means of a Rigaku diffractometer equipped with a nickel-filtered CuK α_1 radiation ($\lambda = 1.5418 \text{ \AA}$).

XPS measurements were performed using a VG Escalab 200R electron spectrometer equipped with a hemispherical electron analyzer and a Mg K α (1253.6 eV) excitation source. Energy corrections were performed using the line of each support as internal reference. The samples were treated as previously stated, cooled to room temperature, flushed with N₂, stored in flasks containing *n*-heptane, and transferred into the pretreatment chamber of the spectrometer. The XPS analyses of these samples were categorized as pre-reaction. After the HDN reaction, the spent catalyst was transferred into flasks containing *n*-dodecane, and analyzed by XPS. The intensity of the peaks was estimated by calculating the integral of each peak after subtracting an S-shaped background and fitting the experimental curve to a combination of Gaussian/Lorentzian lines.

2.3 Catalytic tests

The HDN of quinoline was carried out in an autoclave reactor operating in batch mode. The liquid reactant feed, consisting of quinoline (0.232 mol L⁻¹) in decahydronaphthalene (decaline) (80 mL) with hexadecane (0.0341 mol L⁻¹) as internal standard, was introduced into the reactor. Then, approximately 0.200 g of the selected catalyst was added. As previously indicated, the ReS₂(x)/supports were prepared from the *ex situ* sulfidation and quickly transferred to the reactor to prevent oxidation. The system was closed, and N₂ was bubbled through the solution for 20 min with a flow of 100 mL min⁻¹ to purge any air in the system. Still under N₂ atmosphere, the reactor was heated to the reaction temperature of 573 K with stirring. The reaction timer was initiated when the reaction temperature was reached and the pressure was adjusted to 5 MPa by H₂. The pressure was kept constant during the course of the experiment. Condensed samples were taken periodically during the reaction and quantified by a gas chromatograph (Perkin-Elmer - Clarus 400) equipped with a Flame Ionization Detector (FID) and a CP-Sil 5 column (Agilent, 30 m x 0.53 mm x 1.0 μm film thickness).

The specific rate for the total conversion of quinoline was deduced from the initial slope of conversion as a function of time plot according to the following equation:

$$r_s = \frac{[b \times n]}{m} \quad \text{Eq. (1)}$$

where r_s is the specific rate (mol g⁻¹s⁻¹), b represents the initial slope of the conversion vs. time plot (dimensionless), n is the initial moles of quinoline (mol), and m is the mass of catalyst (g). The intrinsic rate was calculated from the specific rate according to the following equation:

$$r_i = \frac{r_s}{n_{\text{Re}}} * N_{\text{av}} \quad \text{Eq. (2)} \quad \text{where } r_i \text{ is}$$

the intrinsic rate (represent the molecules of quinoline transformed per Re atom and second; and it is expressed as molec. Re at⁻¹ s⁻¹), and r_s is the specific rate (expressed as moles of quinoline transformed per gram of catalyst per second [mol. g⁻¹ s⁻¹]), n_{Re} represents the number of Re atoms per gram of catalyst, and N_{av} is the Avogadro number.

The selectivities (%) were determined at 40% of quinoline conversion, according to Eq. (2):

$$S\% = \frac{X_i}{X_T} \times 100 \quad \text{Eq. (2)}$$

where X_i is the percentage of product formation i , and X_T is the quinoline conversion.

3. RESULTS AND DISCUSSION

3.1 Characterization of catalysts

Figure 1 shows the N₂ adsorption-desorption isotherms of the supports. According to IUPAC classifications, all the isotherms belong to type IV which is typical of mesoporous materials [19]. Also, Fig. 1 shows that the γ -Al₂O₃ and ZrO₂ supports displayed a hysteresis loop, closely resembling a type H1, due to capillary condensation which is typically associated to non-interconnected ink-bottle pores. Meanwhile, the TiO₂ and SiO₂ supports displayed a hysteresis loop resembling a type H3, suggestive of slit-shaped pores. The N₂ adsorption-desorption isotherms of the catalysts (not shown here) were similar to their respective supports. The textural properties from N₂ adsorption-desorption isotherms of the supports and catalysts are summarized in Table 1. The γ -Al₂O₃ support possessed the highest surface area, followed by SiO₂, TiO₂ and ZrO₂ supports. Also, there was a slight decrease in textural properties of the supports (surface area and the total, micropore and mesopore pore volumes) after Re impregnation, suggesting that pore mouth blockage was practically absent.

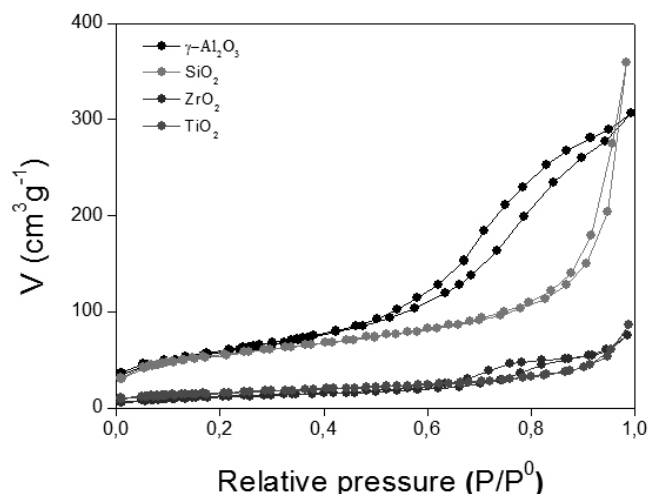


Figure 1: Nitrogen adsorption – desorption isotherms of supports.

Figure 2 shows the XRD patterns of the calcined Re/support catalysts. The patterns obtained were compared to JCPDS data files for phase identification (ReO₄⁻: 010-0252, ReO₃: 041-0967, TiO₂: 01-086-1157; SiO₂: 01-087-0710, ZrO₂: 037-1484, Al₂O₃: 010-0425). Figure 2a and 2b shows the presence of ReO₄⁻ (main peaks 2 θ = 16.7; 25.4; 27.6; 30.4; 40.6; 41.3; 43.48; 47.2; 49.2; 50.9; 52.2) and ReO₃ (main peaks 2 θ = 34.8; 37.9; 59.0; 82.4; 85.5) species over SiO₂ support. Also, it can be observed in Figs. 2a and 2b that the intensity of the ReO₄⁻ peaks was higher than the intensity of the ReO₃ peaks, suggesting that ReO₄⁻ species is the main crystalline phase on this supports, in agreement with Escalona *et al.* [12]. On the contrary, Fig. 2c shows no detected diffraction peaks attributed to ReO₄⁻ and ReO₃ species for the ZrO₂-supported catalysts, suggesting that either ReOx was highly dispersed on this support or that some of the ZrO₂ peaks may have masked the ReOx peaks. Meanwhile, Fig. 2d shows that ReO₄⁻ species was detected on TiO₂ support. Table 1 summarized the crystal size calculated by Scherrer equation. The ReO₄⁻ crystallite size was similar on all supports, around 50 nm. However, this result contradicts a previously reported study by Arnoldy *et al.* [20]; they found by XRD that the ReOx particles size supported on Re(2.5)/SiO₂ and Re(2.43)/ γ -Al₂O₃ catalysts was around 200 nm. This difference in ReOx particles size can be attributed to the impregnation method used by Arnoldy *et al.* [20]. They used several pore volume impregnation steps to reach high Re content, suggesting that this procedure favor the formation of larger ReOx particles size.

Table 1. Composition, textural properties and crystal size obtained from X-ray diffraction of ReOx(x)/support catalysts.

Samples	Re Content (%)	Re surface density (atoms nm ⁻²)	^a S _{BET} (m ² g ⁻¹)	^b V _p (cm ³ g ⁻¹)	^c V _m (cm ³ g ⁻¹)	^d V _o (cm ³ g ⁻¹)	^e ReO ₄ ⁻ Crystal size (nm)
γ-Al ₂ O ₃	---	---	211	0.55	0.46	0.09	---
Re(1.5)/γ-Al ₂ O ₃	9.8	1.5	202	0.35	0.25	0.09	50
ZrO ₂	--	---	41	0.09	0.07	0.02	---
Re(1.5)/ZrO ₂	2.1	1.5	40	0.07	0.05	0.02	n.d.
SiO ₂	---	---	187	0.31	0.22	0.09	---
Re(1.5)/SiO ₂	8.7	1.5	144	0.26	0.19	0.06	47
TiO ₂	---	---	54	0.09	0.06	0.03	---
Re(1.5)/TiO ₂	2.3	1.5	45	0.08	0.06	0.02	56*

^a Determined from BET equation.

^b Calculated from the amount adsorbed at a relative pressure of 0.96.

^c Determined from Dubinin–Radushkevich (D–R) equation.

^d Difference between V_p and V_{p'}.

^e ReO₄⁻ crystal size determined from Scherrer equation using 2q = 25.4°

* ReO₄⁻ crystal size was calculated using 2q = 16.7°

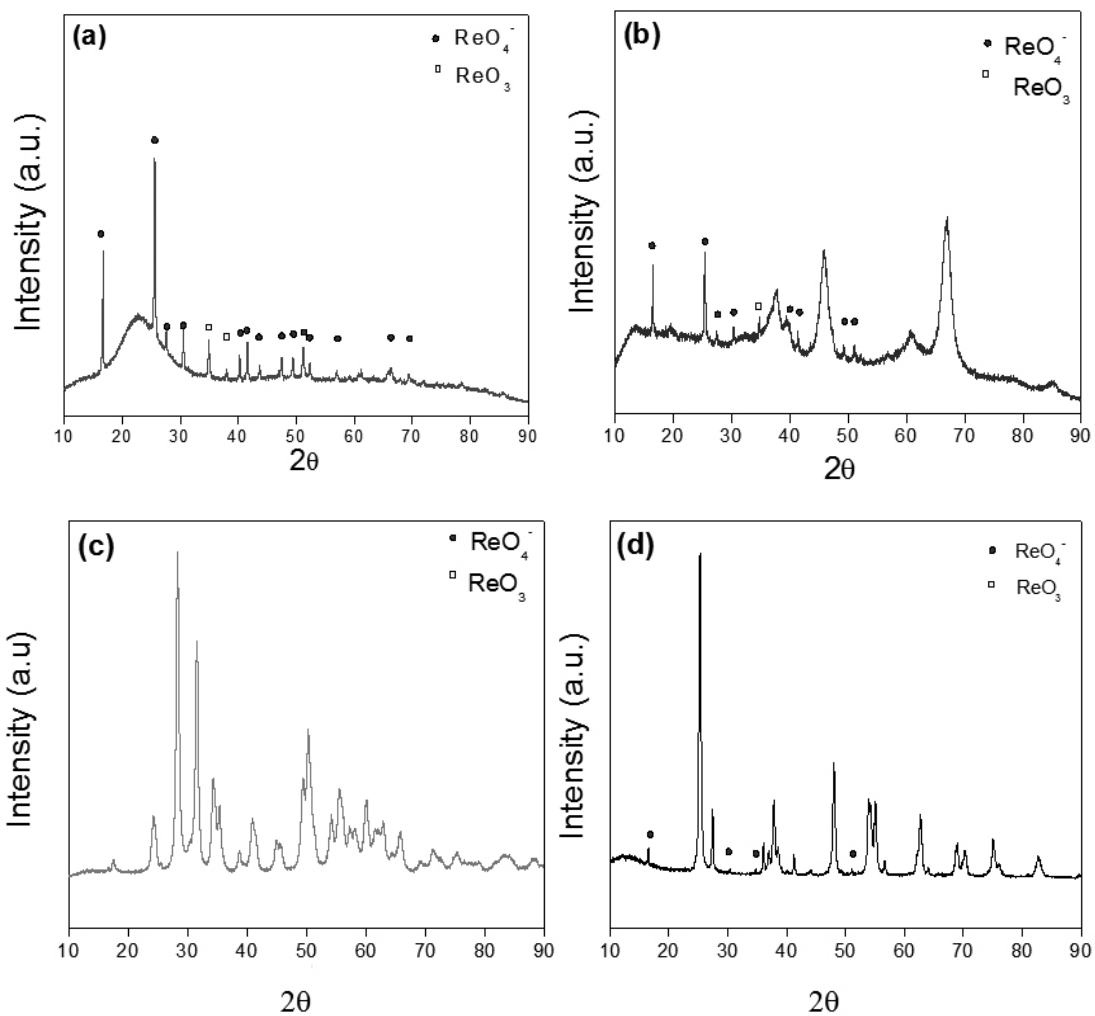
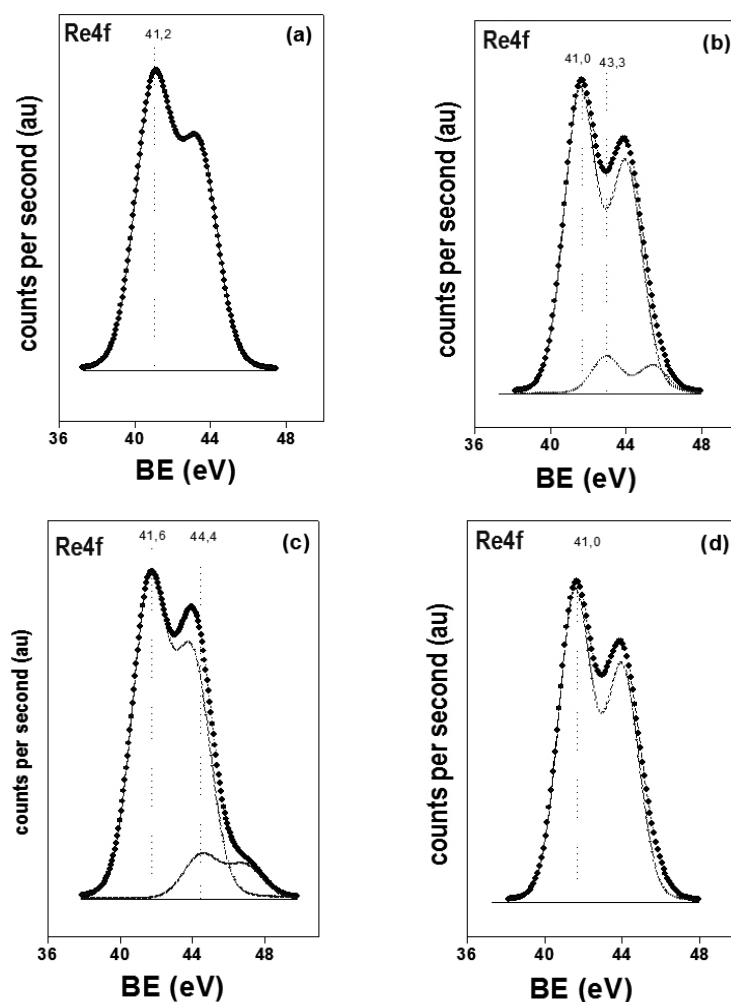
**Figure 2:** X-ray diffraction of a) Re/SiO₂, b) Re/γ-Al₂O₃, c) Re/ZrO₂ and d) Re/TiO₂ catalysts.

Table 2. XPS binding energies (eV) and surface atomic ratios of sulfided catalysts.

Catalysts	M 2p (Si, Al, Zr, Ti) (e.V.)	Re4f _{7/2} (e.V.)	S2p (e.V.)	Re/M at
ReS ₂ (1.5)/SiO ₂	103.4	41.2	161.8	0.041
ReS ₂ (1.5)/ γ -Al ₂ O ₃	74.5	41.6 (89) 43.3 (11)	162.0	0.034
ReS ₂ (1.5)/ZrO ₂	182.2	41.6 (88) 44.4 (12)	162.0	0.028
ReS ₂ (1.5)/TiO ₂	458.6	41.0	161.7	0.089

Figure 3 shows the XPS spectra of Re/support catalysts with a surface density of 1.5 atoms of Re per nm² of supports. Curve fitting of spectra in Figures 3a and 3d revealed one doublet, each one containing the Re 4f_{7/2} and Re 4f_{5/2} peaks, indicating the presence of one Re species. Meanwhile, curve fitting of the spectra in Fig. 3b and 3c shows two partially overlapping doublets containing the Re 4f_{7/2} and Re 4f_{5/2} peaks, indicating the presence of two Re species. Table 2 summarizes the binding energies (BE) of the most intense Re 4f_{7/2} component of each doublet, its relative proportions (between parentheses) and surface atomic ratio for Re/supports catalysts. Table 3 shows that the Re 4f_{7/2} components of the most intense doublet remained constant in all the catalysts, at about 41.4 eV \pm 0.3, and corresponds closely to the values reported

for ReS₂ [12, 21, 22]. A single peak for S 2p peaks at 162 eV \pm 0.4 indicates the presence of S²⁻ for all the sulfided catalysts. The BE of the Re 4f_{7/2} peaks of the less intense doublet displayed by Re/ γ -Al₂O₃ and Re/ZrO₂ catalysts was around 43.9 eV \pm 0.3, which can be assigned to Re oxysulfide species [12, 13, 21, 22]. These results indicate that Re sulfidation was slightly incomplete, and that the procedure used led to an estimated 90 % sulfidation for γ -Al₂O₃- and ZrO₂-supported catalysts. This result suggests a strong interaction between ReOx species and these supports. On the other hand, the Re/TiO₂ and Re/SiO₂ catalysts displayed only a component of the Re 4f_{7/2} peak, indicating complete Re sulfidation.

**Figure 3:** XPS of sulfides: a) Re/SiO₂, b) Re/ γ -Al₂O₃, c) Re/ZrO₂ and d) Re/TiO₂ catalysts.

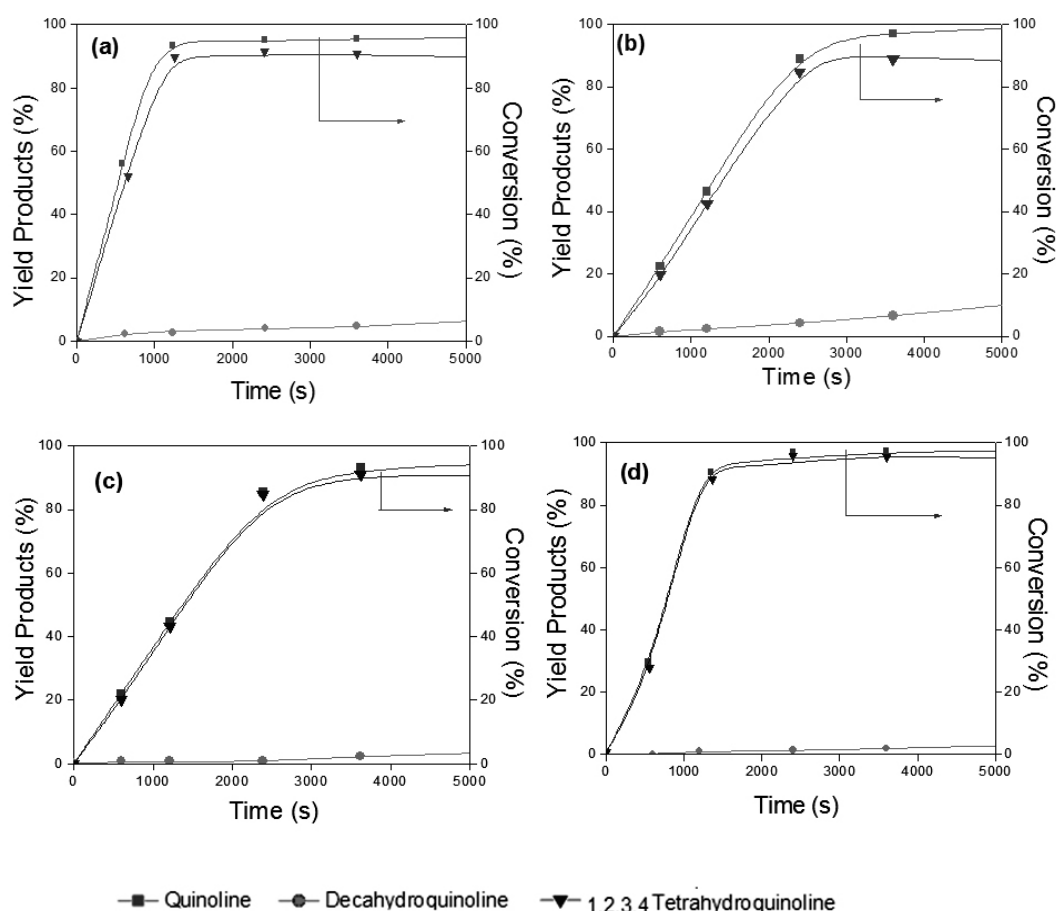


Figure 4: Quinoline conversion and yield of products over a) Re/SiO₂, b) Re/γ-Al₂O₃, c) Re/ZrO₂ and d) Re/TiO₂ catalysts.

Table 2 also shows that Re/M atomic ratios for the ReS₂/supports catalysts. This shows that Re/TiO₂ catalysts displayed the highest Re/M atomic ratios, followed by Re/SiO₂, Re/γ-Al₂O₃ and Re/ZrO₂ catalysts. This trend suggests that ReS₂ was most highly dispersed on the TiO₂ support, while it was poorly dispersed on the ZrO₂ support, as previously observed by Laurenti *et al.* [14]. Unfortunately, HRTEM cannot be used to estimate the size of sulfide because the lamellar structure decomposes into spherical metallic particles under electron beam [14].

1.2 Catalytic activity of catalysts

Figure 4 illustrates the conversion of quinoline and yield of products over ReS₂/support catalysts as a function of time. It can be observed that the main reaction product was 1,2,3,4 tetrahydroquinoline (THQ1), and that decahydroquinoline (DHQ) was observed in minor amounts for all the catalysts. The conversion of quinoline by the ReS₂(x)/supports catalyst can be depicted in the reaction scheme shown in Figure 5, in agreement with previously reported studies by several authors [4, 5, 6, 9, 10]. Figure 5 shows that the formation of DHQ compound can be produced through hydrogenation of quinoline (either via THQ1 or THQ5 intermediate compounds). However, THQ5 was not detected under the experimental conditions used. Figure 6 illustrates the products distribution calculated at 40 % of quinoline conversion.

The Re/SiO₂ and Re/γ-Al₂O₃ catalysts displayed a higher yield to DHQ compound than the Re/ZrO₂ and Re/TiO₂ catalysts, suggesting that SiO₂ and γ-Al₂O₃ supports slightly modified the active sites favouring the hydrogenation route. In this sense, Laurenti *et al.* [14] studied the HDS of thiophene over Re/ZrO₂, Re/TiO₂ and Re/γ-Al₂O₃ catalysts, and suggested the formation of ReS₂(x) under the reaction condition used. In other words, the authors proposed the formation of a metallic character in ReS₂. In fact, C. Sepulveda *et al.* [23] demonstrated by kinetic approach of competitive hydrogenation the presence of a metallic character on ReS₂ supported on SiO₂ and γ-Al₂O₃. Therefore, the higher yield to DHQ displayed by Re/SiO₂ and Re/γ-Al₂O₃ catalysts could be attributed to higher ReS₂ metallic character on these supports.

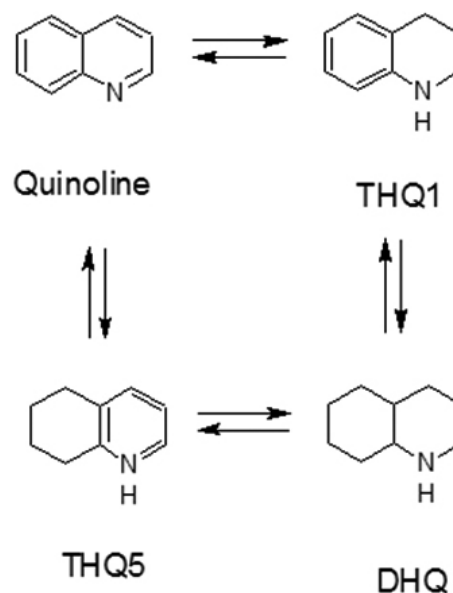


Figure 5: Reaction network for the conversion of quinoline.

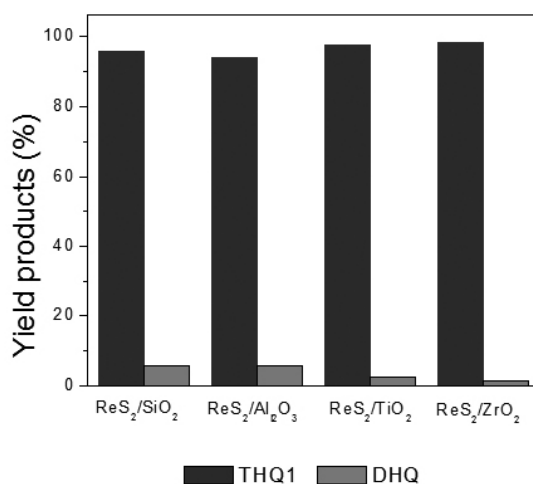


Figure 6: Products distribution at 40% conversion of quinoline for ReS₂(x)/supports catalysts.

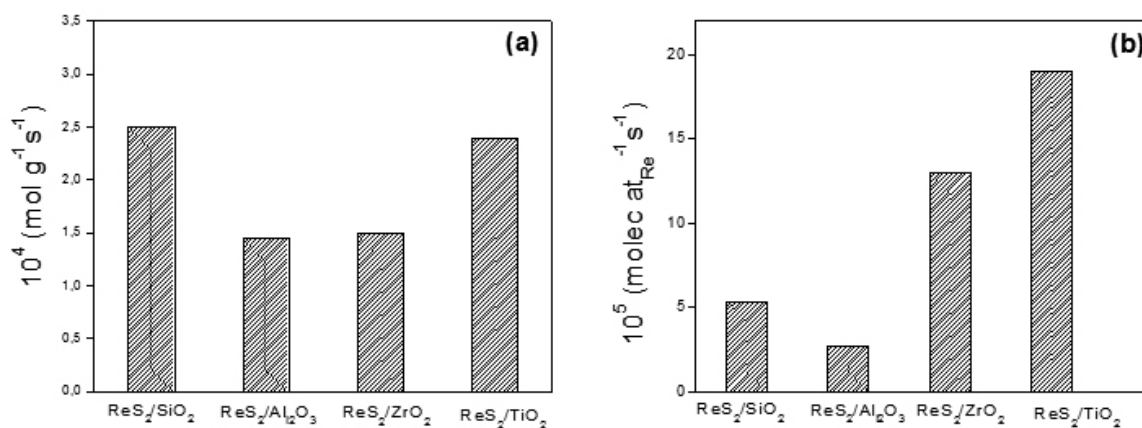


Figure 7: a) Specific rate and b) intrinsic rate of ReS₂(x)/supports catalysts.

The negligible formation of N-free compounds observed for the Re/support catalysts contrasts with the results reported recently by Fagar *et al.* [24] in the HDN of quinoline over MoS₂ catalyst. The MoS₂ displayed high selectivity to THQ1 and C9 products. This behaviour can be due to an inhibitive effect similar to those observed in the HDN of indole [25] and carbazol [26]. Laredo *et al.* [25] studied, by kinetic approach mechanism, the inhibition of indole and o-ethylaniline in the HDS of difenzothiophene (DBT) over commercial Co-Mo/ γ -Al₂O₃ catalyst at conditions commonly used in the hydrotreatment of diesel feedstock. They observed an unexpected self-inhibiting effect of indole and o-ethylaniline in their hydrogenation process during DBT HDS. Similar self-inhibitive effect was observed in the HDN of carbazol and the HDS of DBT over Ni-MoP/ γ -Al₂O₃ commercial catalyst [26]. These results suggest a possible retardation in the formation of N-free compounds in the batch reactor. In fact, reaction of these same catalysts in continuous flow reactor (elimination of self-inhibiting effect) showed high formation of N-free compounds (data not show here).

Figure 7 shows the activity expressed as the initial rate (per gram of catalysts) and intrinsic initial rate (by metal atom) of all the catalysts evaluated in this study. Fig. 7a shows that the Re/SiO₂ catalyst displayed the highest initial rate followed by Re/Al₂O₃, Re/ZrO₂ and Re/TiO₂ catalysts. This behaviour can be a function of Re atoms surface loading due to differences in the surface area of supports. Regarding the intrinsic activity, Fig. 7b shows that the ReS₂/TiO₂ catalyst displayed the highest intrinsic activity, followed by Re/ZrO₂, Re/SiO₂ and Re/ γ -Al₂O₃ catalysts. Similar trend was observed previously by Laurenti *et al.* [14] in the conversion of thiophene. The highest intrinsic activity observed over the Re/TiO₂ catalyst can be attributed to higher ReS₂ dispersion on the

TiO₂ support, as suggested by XPS. On the contrary, the lower intrinsic activity displayed by Re/ γ -Al₂O₃ catalysts cannot be correlated with XPS results. This catalyst presented a similar ReS₂ dispersion to the Re/ZrO₂ catalyst; however, the Re/ZrO₂ catalyst displayed an intrinsic activity about 4.5 times higher than the Re/ γ -Al₂O₃ catalyst. These results did not show a clear correlation between the catalytic activity and the structure of the γ -Al₂O₃-, ZrO₂- and SiO₂-supported ReS₂ catalysts, suggesting that other factors are involved in the conversion of quinoline, such as the existence of an electronic effect induced on the active phase by the support. Laurenti *et al.* [14] and Sepulveda *et al.* [23] reported the formation of ReS_(2-x) species under reaction condition over SiO₂, γ -Al₂O₃- and ZrO₂-, while over TiO₂ catalyst apparently this specie was not formed. Therefore, the formation of ReS_(2-x) over γ -Al₂O₃, ZrO₂ and SiO₂ supports could favor the HYD pathway but decrease the quinoline conversion. This behavior contrasts results previously observed for the conversion of thiophene, suggesting that this species disfavor the adsorption of quinoline over the active site. However, in the case of ZrO₂ support the intrinsic rate was higher than Re/SiO₂ and Re/ γ -Al₂O₃ catalysts, this behavior is not clear. Future research should be aimed at clarifying this possible electronic effect (exact ReOx nature) versus Re dispersion on the HDN reaction over this active phase.

4. CONCLUSIONS

The ReS₂(1.5)/supported catalysts are highly active in the conversion of quinoline but exhibit negligible activity on the formation of N-compounds in a batch reactor. This behavior was attributed mainly to a self-inhibitive effect by some of the products from quinoline conversion in the batch reactor.

The highest activity presented by the $\text{ReS}_2/\text{TiO}_2$ catalyst was attributed to the combined effect of Re dispersion and the formation of ReS_2 species. Meanwhile, the activity trends displayed over the $\text{Re}/\gamma\text{-Al}_2\text{O}_3$, Re/SiO_2 and Re/ZrO_2 catalysts cannot be related to any structural and textural properties of the catalysts, suggesting that the support can be involved in modifying the active site by electronic effect. The Re/SiO_2 and $\text{Re}/\gamma\text{-Al}_2\text{O}_3$ catalysts displayed a higher yield to DHQ compound than the Re/ZrO_2 and Re/TiO_2 catalysts. The results were attributed to higher ReS_2 metallic character over Re/SiO_2 and $\text{Re}/\gamma\text{-Al}_2\text{O}_3$ catalysts favouring of yield to DHQ compound but decreasing the quinoline conversion.

ACKNOWLEDGMENTS

The authors thank CONICYT-Chile for FONDECYT N° 1130749 grant.

REFERENCE

- 1.- Liu C, Yu Y, Zhao H, Fuel Processing Technology **25**, 449 (2005)
- 2.- Fang M, Tang W, Yu C, Xia L, Xia Z, Wang Q, Luo Z, Fuel Processing Technology **129**, 236 (2015).
- 3.- Ho T. C., Catal. Rev. Csi. Eng **30**, 117 (1988).
- 4.- Deepa G, Sankaranarayanan T.M, Shanthi K, Viswanathan B., Catal. Today **198**, 252 (2012).
- 5.- Yang S.H and Satterfield C.N., Ind. Eng. Chem. Process Des. Dev. **23**, 20 (1984).
- 6.- Moreau C, Bekakra L, Durand R and Geneste P., Catal. Today **10**, 681 (1991).
- 7.- Laredo G.C, Altamirano E, De los Reyes J.A. Appl. Catal A: Gen. **243**, 207 (2013).
- 8.- Kabe T, Ishihara A, Qian W (1999) Hydrodesulfurization and Hydrodenitrogenation, in: Chemistry and Engineering, Wiley-VCH-Verlag and Kodansa, Tokyo.
- 9.- Chouzier S, Vrinat M, T Cseri, Roy-Auberger M, Afanasiev P. Appl. Catal A:Gen **400**, 82 (2011).
- 10.- Eijsbouts S, De Beer V.H.J, Prins R., J. Catal **127**, 619 (1991).
- 11.- Escalona N, Vrinat M, Laurenti D, Gil Llambías F. J., Appl. Catal. A:Gen **322**, 113 (2007).
- 12.- Escalona N, Ojeda J, Cid R, Alvez G, López Agudo A, Fierro J.L.G, Gil-Llambías F.J. Appl. Catal. A:Gen **232**, 45 (2002)
- 13.- Escalona N, Ojeda J, Yates M, Lopez Agudo A, Fierro J.L.G and Gil-Llambías F. J. Applied. Catal. A:Gen **240**,151 (2003).
- 14.- Laurenti D, Thoa K.T, Escalona N, Massin L, Vrinat M, Gil Llambías F. J. Catal Today **130**, 50 (2008).
- 15.- Cáceres C.V, Fierro J.L.G, Lázaro J, López Agudo A, Soria J., J. Catal. **122**, 113 (1990)
- 16.- Hédoire C.-E, Louis C, Davidson A, Breyse M, Maugé F, Vrinat M., J. Catal. **220**, 433 (2003).
- 17.- Breyse M, Afanasiev P, Geantet C, Vrinat M., Catal. Today **86**, 5 (2003)
- 18.- Laurenti D, Phung-Ngoc B, Roukoss C, Devers E, Marchand K, Massin L, Lemaitre L, Legens C, Quoineaud A.-A, Vrinat M., J. Catal. **297**, 165 (2013).
- 19.- Brunauer S, Deming L, Deming W. E, Teller E. J. Am. Chem. Soc. **62**, 1723 (1940).
- 20.- Arnoldy P, Van Oers E. M, Bruinsma O. S. L, De Beer V. H. J, Moulijn J. A. Journal of Catalysis **93**, 231 (1985).
- 21.- Leiva K, Martínez N, Sepulveda C, García R, Jiménez C. A, Laurenti D, Vrinat M, Geantet C, Fierro J. L. G, Ghampson I. T, Escalona N., Appl. Catal A:Gen **490**,71 (2015).
- 22.- Leiva K, Sepulveda C, García R, García J. L, Escalona N., Catal. Comm **53**, 44 (2014).
- 23.- Sepulveda C, García R, Escalona N, Laurenti D, Massin L, Vrinat M, Catal Lett **141**, 987 (2011).
- 24.- Farag H, Kishida M, Al-Megren H, Applied Catalysis A: Gen **469**, 173 (2014).
- 25.- Laredo G.C, Altamirano E, De los Reyes J.A, Applied Catalysis A: Gen **242**, 311 (2003).
- 26.- Laredo G. C, Montesinos A, De los Reyes J. A, Applied Catalysis A: Gen **265**,171 (2004).